IJCB
INDONESIAN JOURNAL OF COMPUTATIONAL BIOLOGY

Research Article
Vol.2 No.1 (2023), 11-21

Computational Simulation of Indonesian Natural Compounds as Main Protease Inhibitors of SARS-CoV-2

Setyanto Tri Wahyudi[1,3,*], Zahra Silmi Muscifa[1,4], Tony Sumaryada[1], and Laksmi Ambarsari[2]

1. Department of Physics, Faculty of Mathematics and Natural Sciences, IPB University, 16680

2. Department of Biochemistry, Faculty of Mathematics and Natural Sciences, IPB University, 16680

3. Tropical Biopharmaca Research Center, Institute of Research and Community Services, IPB University, Indonesia 16128

4. Research Center for Molecular Biotechnology and Bioinformatics, Universitas Padjadjaran, Indonesia 40132

** Corresponding Author : stwahyudi@apps.ipb.ac.id*

***Received**: March 24, 2023; **Accepted**: May 19, 2023; **Available Online:** July 17, 2023*

The computational method provides an alternative approach for conducting screening of natural substances' antiviral properties against the SARS-CoV-2 virus. This research focuses on the main Protease, a target protein that plays a central role in viral replication by producing an enzyme that cleaves the host protein nuclear factor (NF)-κB in SARS-CoV-2. The study used a thousand natural compound structures from the Indonesian Natural Compound Database (Herbaldb), filtered based on the similarity of their pharmacophore features with main protease inhibitors. In compounds with good pharmacophore properties, docking will be carried out to determine the binding affinity with the target protein and obtain the complex structure. The ADMETSAR test determined the pharmacology and pharmacokinetics of the five best natural compounds. Finally, a molecular dynamics simulation of the complex structure was performed to assess the stability of the best compound interactions with the SARS-CoV-2 main protease. The compounds identified as the main protease inhibitors in this study were cosmosiin, glucobrassicin, and isobavachin.

Keywords: ADMETSAR test | docking | molecular dynamic simulation | Indonesian natural compound | SARS-CoV-2.

Computational drug discovery provides an alternative approach for computer simulation-assisted screening of drug candidate compounds, which can significantly reduce research time and costs. Computer-based research uses pathogen characteristics of the antiviral targets being developed. This research aims to discover a natural compound-derived antiviral against SARS-CoV-2[1].

The target protein used in this study is the main protease of SARS-CoV-2, which cuts the host protein nuclear factor (NF)-κB essential modulator (NEMO). NEMO is involved in signalling cascades that regulate the transcription of many genes, including antiviral type I interferon and other immune genes. Besides gene regulation, NEMO modulates cell survival[2]. The main Protease of SARS-CoV-2 is highly conserved across different strains of the virus. This conservation makes it an attractive target for drug development because a drug designed to inhibit the main Protease is likely effective against various viral strains[3]. Inhibiting the main protease of SARS-CoV-2 can stop the process of replication and transmission of SARS-CoV-2[4]. The main protease structures used in the study were downloaded from the protein data bank (PDB) (https://www.rcsb.org/). Previous studies focused on screening herbal compounds for COVID-19 have identified potential compounds with inhibitory properties against the main protease of SARS-CoV-2.

This finding signifies the potential of natural compounds derived from herbal sources to serve as effective treatments against COVID-19[5]. The natural compound used in the virtual screening stage as an inhibitor for SARS-CoV-2 comes from the Indonesian natural compound database (Herbaldb)[6], while the 3D structure is downloaded from PubChem (https://pubchem.ncbi.nlm.nih.gov/). In the first stage, structure-based virtual screening was carried out with the liganddScout 4.4 (which offers a one-month free trial) to obtain similarities in the pharmacochemical features of natural compounds with co-crystallized ligands from the main protease structure.

The next stage involves docking to obtain affinity energy and active site interactions of natural compounds-main protease. The ADMETSAR test[7] will evaluate natural compounds with the highest affinity energy, revealing their potential pharmacological and pharmacokinetic properties as drug candidates. Finally, molecular dynamics simulations will be carried out on the structure of the natural compound-main protease complex to determine its stability.

Methods

Exploring Natural Active Compounds Databased

The first stage involves exploring a 3D structure database of natural compounds with potential bioactivity against viruses, bacteria, and cancer cells. These compounds are sourced from the Indonesian natural compound database HerbalDB (http://herbaldb.farmasi.ui.ac.id/v3/). The 3D structures of these compounds are downloaded from the PubChem web server (https://pubchem.ncbi.nlm.nih.gov/), which provides 3D structures of chemical compounds. The collected natural compounds are structured and optimized using ORCA software[8]. Optimization with ORCA refines the molecule's geometry to find its most stable conformation or the transition state for a specific reaction. Optimization is a critical step in computational chemistry as it ensures that the molecular structure is energetically optimized and in a minimum energy state.

.

DOI: https://doi.org/10.24198/ijcb.v2i1.46021

Virtual screening procedure for Structural Based and Docking of SARS-CoV-2 with Natural Active Compounds

After optimization with ORCA, the natural active compounds will be used as ligands for screening pharmacophore-based compounds. At this stage, natural compounds will be selected based on their pharmacophore features similar to the co-crystalized ligands in the main protease structure of SARS-CoV-2. The docking of compounds with similar pharmacophore features into the main protease structure will be performed using Autodock Vina and Autodfoock 4. The 3D structures of natural compounds and co-crystallized ligands will be prepared as pdbqt extensions for docking at the active site of the main protease, which is set at 15 x 15 x 15 Å with the center points x = -12.04, y = 11.23, and z = 68,48. The best potential compounds will undergo evaluation using the Lipinski rule of five and toxicity testing with the ADMETSARsar web server, which employs the ADMETSAR method (absorption, distribution, metabolism, excretion, and toxicity, to determine their efficacy and safety.

Molecular Dynamics Simulation

The initial preparation stage resulted in a complex file formed by the docking process between the SARS-CoV-2 protein and the active natural compound with the best affinity value. The lower binding energy values indicate good stability in complex compounds, making it the best affinity. The complex structure files are assigned an AMBER ff14sb force field[9], and then they load a solvent box measuring 20×20×20 Å. The simulation system preparation is carried out with the help of a tleap program.

Energy Minimization

The minimization stage aims to minimize the energy of the complex structure so that it resembles its natural state, avoids inappropriate van der Waals contacts (bad contact), and minimizes high-energy steric effects. Minimization is carried out in stages with different restraints, that is 1000, 500, 250, 100, and 50 kcal/mol. In the end, the restraint is removed and the molecules move freely.

Heating and Equilibration

The heating stage of this procedure uses the Langevin protocol and the NVT dynamic ensemble. The system is heated to a temperature of 300 K while being restrained at 10 kcal/mol to prevent the molecules of the complex structure from moving until the target temperature is reached. The restraint is gradually removed during the equilibration stage, allowing the system to adjust to the given temperature.

Production Run and Analysis

The NPT method's equilibration results were further analyzed by running a 50-ns molecular dynamics simulation using 25 separate scripts with a timestep of 2 fs. After the simulation, various analyses were performed, including Root Mean Square Deviation (RMSD), Root Mean Square Fluctuation (RMSF), hydrogen-bonding interactions, and MMPBSA energy calculation[10].

Result and discussion

Selection of Structures and Active Sites

The Protein Data Bank (https://www.rcsb.org/) contains several main protease structures with high resolution, including 6M0K (resolution: 1.504 Å) with FJC inhibitor (11b), which has been shown to inhibit Mpro SARS-CoV-2 in cell culture[11]; 7D1M (resolution: 1.35 Å) with GC376 inhibitor, which is an inhibitor of the feline coronavirus[12]; and 6Y2F (resolution: 1.95 Å) with alpha-ketoamide inhibitor[13]. Each structure was re-docking with its respective inhibitor. Table 1 shows, that the 7D1M structure, has the most negative affinity energy. This is because 7D1M has the best resolution and completeness of its constituent amino acid residues. This study will use 7D1M chain A as the Mpro receptor.

Table 1 Binding Energy of Comparison Ligands on Structures

Ligand	Repeating	6M0K resolution: 1.5 Å		7D1M resolution 1.4 Å		6Y2F resolution1.95 Å		Ligand Affinity
		Chain A	Chain B	Chain A	Chain B	Chain A	Chain B	
FJC (Ligand 6M0K)	1	-7.6	-7.7	-9	-8.2	-7.9	-7.9	-8.01
	2	-7.6	-7.6	-9	-8.1	-7.9	-7.9	
	3	-7.3	-7.4	-8.9	-8.3	-7.9	-7.9	
	Average	-7.5	-7.57	-8.97	-8.2	-7.9	-7.9	
GC376 (Ligand 7D1M)	1	-6.3	-6.1	-7	-7.5	-6.8	-6.3	-6.81
	2	-6.5	-6.5	-7.3	-7.7	-7	-6.7	
	3	-6.1	-6.3	-7.2	-7.5	-6.7	-7	
	Average	-6.3	-6.3	-7.17	-7.57	-6.83	-6.67	
Alfa-ketoamide (Ligand 6Y2F)	1	-6.6	-6.6	-7.8	-7.5	-7.3	-7.2	-7.1
	2	-7	-6.7	-7.4	-7.5	-7	-7.2	
	3	-6.4	-6.4	-7.6	-7.5	-7.1	-7	
	Average	-6.67	-6.57	-7.6	-7.5	-7.13	-7.13	
Affinity of Structure		-6.82	-6.81	**-7.91**	-7.76	-7.29	-7.23	

http://jurnal.unpad.ac.id/ijcb

DOI: https://doi.org/10.24198/ijcb.v2i1.46021

Structure Based Virtual Screening and Docking Simulation

The next step is to carry out virtual screening using structure-based based on the similarity of the pharmacophore features of 1000 natural ingredients to the three inhibitors contained in the LigandScout-assisted structure. The structure-based virtual screening stage considers the steric and electronic features of the inhibitors and compares them with the structure of natural materials. Table 2 shows that the FJC inhibitor (11b) has two hydrophobic interactions **(columns 1-2)**, three hydrogen bond acceptors **(columns 3-6)**, and three hydrogen bond donors **(columns 7-10)**. Fifty-two natural compounds share five pharmacophore features in common with FJC (11b). The next stage involves virtual screening docking of these 52 natural product compounds. Seven compounds were found to have better affinity energy when compared to FJC (Table 2). This affinity energy was obtained using AutoDock Vina.

Another inhibitor that can inhibit the main protease of SARS-CoV-2 in vitro is Alfaketoamide. Table 3 shows that alpha-ketoamide has two hydrophobic interactions **(columns 1-2)**, four hydrogen bond acceptors **(columns 3-6),** and seven hydrogen bond donors **(columns 7-13)**. Thirty-three compounds have at least five pharmacophore features in common with alpha-ketoamide. The docking using AutoDock-Vina produced sixteen natural product compounds that have a better energy affinity than alpha-ketoamide. The affinity energy value of molecular docking can predict the ligand-protein's intermolecular interaction and the ligand's inhibitory ability to stop the main protease's activity[14] meanwhile, in our database, no natural product compounds were found to possess the same pharmacophore features as GC376.

Table 2 Docking of natural product compounds that have similar pharmacophore features with FJC

No	Compound or Pubchem ID	Pharmacophore feature										Energy Affinity (kcal/mol)
		1	2	3	4	5	6	7	8	9	10	
1	10621		✓	✓	✓	✓	✓		✓			-9.2
2	44258477		✓	✓	✓	✓	✓					-9
3	44257872	✓			✓	✓	✓			✓		-8.5
4	5316261	✓	✓	✓	✓	✓	✓					-8.4
5	42607834			✓	✓	✓	✓					-8.4
6	13845917	✓		✓	✓	✓	✓					-8.3
7	193679		✓	✓	✓	✓	✓		✓			-8.3
8	FJC	✓	✓	✓	✓	✓	✓	✓	✓	✓	✓	-8.2

Table 3 Docking of natural product compounds that have similar pharmacophore features with Alpha ketoamide

No	Compound or Pubchem ID	Pharmacophore feature												Energy Affinity (kcal/mol)
		1	2	3	4	5	6	7	8	9	10	11	12	
1	5280704			✓	✓	✓		✓	✓	✓			✓	-8.8
2	10621			✓	✓	✓		✓	✓	✓				-8.7
3	65065		✓	✓	✓	✓		✓		✓				-8.6
4	15595751				✓	✓	✓		✓		✓			-8.6
5	5280804		✓	✓	✓				✓	✓	✓			-8.6
6	42607834			✓	✓	✓	✓		✓					-8.4
7	5481882			✓	✓	✓	✓							-8.2
8	442416		✓	✓	✓	✓						✓	✓	-8.2
9	5280804		✓	✓	✓	✓			✓		✓			-8
10	5319221		✓	✓	✓	✓		✓		✓				-7.6
11	11948668	✓		✓	✓		✓		✓		✓			-7.5
12	13855735			✓	✓	✓		✓		✓		✓		-7.5
13	9930064	✓		✓	✓	✓		✓		✓				-7.4
14	25085768		✓	✓	✓	✓		✓	✓	✓				-7.4
15	656561			✓	✓	✓		✓	✓	✓				-7.4
16	5280372		✓	✓	✓	✓						✓	✓	-7.3
17	Alfa Ketoamide	✓	✓	✓	✓	✓	✓	✓	✓	✓	✓	✓	✓	-7.2

http://jurnal.unpad.ac.id/ijcb

DOI: https://doi.org/10.24198/ijcb.v2i1.46021

The next step involved molecular docking with the Autodock4 software structure, which identified at least six pharmacophore features in common and demonstrated better affinity energy than the comparison ligands. The selected natural compounds were labeled as LF, which had the same pharmacophore features as FJC, and LAK, which had the same pharmacophore features as an alpha-ketoamide ligand. The Autodock-4 scoring function is semi-empirical, incorporating the Coulomb potential, Leonard Jones potential, system desolvation, and conformational entropy. In contrast, the Autodock-Vina scoring function is empirical, consisting of Gaussian interactions, hydrogen bonding interactions, hydrophobic interactions, and covalent bonds. However, Autodock-4 provides accurate affinity energy values correlating with experimental data[15]. The docking results presented in Table 4 indicate that the ligand co-crystallized from the main protease structure with the strongest binding affinity is FJC (11b), with a binding affinity value of -9.06 kcal/mol, followed by alpha-ketoamide at -7.78 kcal/mol and GC376 at -7.62 kcal/mol. The docking results for the natural compounds produced varied values, but LAK2, LAK5, LAK8, and LAK9 demonstrated better binding affinities than the co-crystallized ligands.

Table 4 Docking Binding Affinity using Autodock4

No	Compound	Energy Affinity (kcal/mol)
1	Alfa Ketoamide	-7.78
2	GC376	-7.62
3	FJC	-9.06
4	5280704 **(LAK1)**	-7.64
5	10621 **(LAK2 and LF1)**	-7.47
6	65065 (**LAK3)**	-7.8
7	5280804 **(LAK4)**	-7.5
8	442416 **(LAK5)**	-7.16
9	5319221 **(LAK6)**	-7.83
10	13855735 **(LAK7)**	-7.78
11	25085768 **(LAK8)**	-4.89
12	656561**(LAK9)**	-6.02
13	5316261**(LF2)**	-9.11
14	193679 **(LF3)**	-8.73

Testing The ADMETSAR Properties

The ligand co-crystalize and the best seven natural compounds go through with ADMET property testing [16], where the best natural compound demonstrated exceptional affinity energy surpassing that of the ligand co-crystalize. The analysis concentrated on five critical ADMET indicators, particularly the Applicability Domain, which comprises six physicochemical and topological properties that dictate a compound's usability, such as molecular weight, alogP, number of atoms, aromatic rings, hydrogen bond donors, and acceptors. Additionally, the analysis included Human Intestinal Absorption, AMES Mutagenesis, carcinogenicity, and LD50 to provide crucial insights into the compound's toxicity, carcinogenic potential, and ability to cause mutations[17].

Table 5 shows that the ligand co-crystalize has ADMET properties that are good enough pharmacologically to be developed as drugs (In domain), namely having a molecular weight in the range 86 to 829, a water partition coefficient in the range -4 to 8.33, atomic number less than 59, the number of aromatic rings is less than seven. It has a maximum of 15 hydrogen acceptors and a maximum of 7 hydrogen donors. Pharmacologically the seven best natural compounds can be developed as drugs (Table 6). Pharmacokinetically, the ligand co-crystalize can enter the gastrointestinal system. The co-crystalized ligand demonstrated no potential to cause cancer or mutations in test bacteria, indicating its safety for potential use in drug development. Table 6 shows that all-natural compounds do not have the potential to cause cancer, but LAK6 and LAK7 cannot enter the body's gastrointestinal system, and LAK4 and LF2 have the potential to cause mutations in the test bacteria. The ADMET test found that LAK1, LAK3 and LF3 were the best compounds to be continued for the binding affinity consistency test using PSO-Vina, which used a combined particle swarm optimization method and Broyden-Fletcher-Goldfarb-Shannon used by auto dock-vina[18].

http://jurnal.unpad.ac.id/ijcb DOI: https://doi.org/10.24198/ijcb.v2i1.46021

Table 5 Properties of ADMET main protease Inhibitor Compounds

ADMET Properties	Alfa Ketoamide	FJC	GC376
Applicability Domain	In Domain	In Domain	In Domain
HIA	(+)0.85	(+)0.92	(+)0.88
Carciogenecity	(-)0.72	(-)0.92	(-)0.88
AMES Mutagenesis	(-)0.6	(-)0.52	(-)0.76
LD50 in Rat (kg/mol)	2.501	1.901	3.838

Table 6 Properties of ADMET main protease Inhibitor Natural Compounds

ADMET Properties	LAK1	LAK3	LAK4	LAK6	LAK7	LF2	LF3
Applicability Domain	In Domain	In Domain	Warning	In Domain	In Domain	In Domain	In Domain
HIA	(+) 0.63	(+)0.99	(+)0.64	(-)0.42	(-)0.43	(+)0.97	(+)0.99
Carciogenecity	(-)0.98	(-)0.98	(-)0.985	(-)0.98	(-) 1	(-)0.85	(-)0.97
AMES Mutagenesis	(-)0.61	(-)0.54	(+)0.81	(-)0.51	(-)0.76	(+)0.7	(-)0.61
LD50 in Rat (kg/mol)	2.69	2.38	3.08	3.37	3.29	2.60	1.76

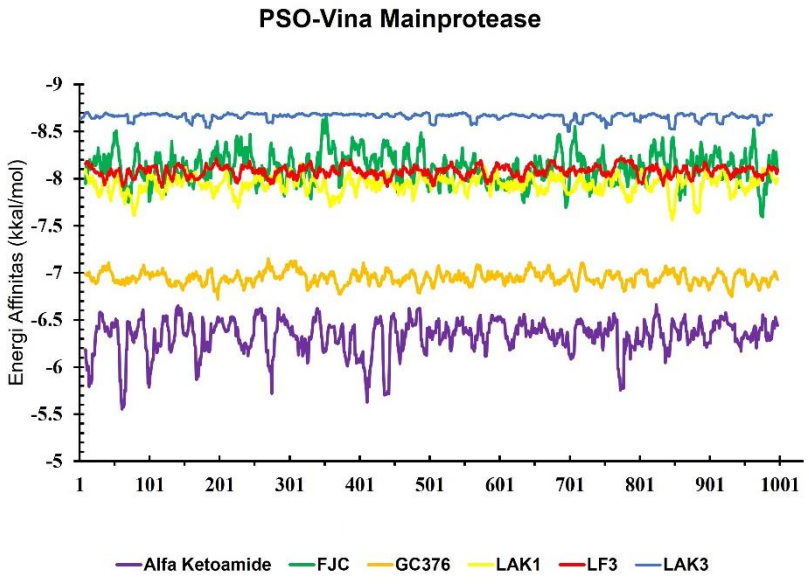

Figure 1 Energy Consistency Affinity of Natural Compounds and Ligands co-crystalize using PSO-Vina in the main protease structure.

http://jurnal.unpad.ac.id/ijcb DOI: https://doi.org/10.24198/ijcb.v2i1.46021

Visual Analysis and Molecular Dynamics Simulation of Main protease Complex Structure

The active site of the main protease of SARS-CoV-2 is located in the cleft between domains I and II and contains the histidine/cysteine catalytic dyad. Cys^{145} acts as a nucleophile during hydrolysis, assisted by His^{41} as a base catalyst. The oxyanion hole, formed by the amido backbone groups of Gly^{143} and Cys^{145} in the oxyanion loop (residues 138–146), stabilizes the partial negative charge of the P1 carbonyl group during hydrolysis of the P1–P1' bond, which is essential for cutting pp1a and pp1ab[19]

The catalytic residues of Mpro SARS-CoV-2 are Cys^{145} and His^{41}, located in the cavity of the active site on the protein's surface. This cavity is a junction of domain 1 and domain 2 of the main protease protein structure. The ligands LAK1, LAK3, and LF3 were visually analysed to investigate their interaction at the center of the protein's active site. The Alpha ketoamide ligand (Figure 2A) contains hydrogen bond donors, acceptors, and hydrophobic interactions. The docking complex structure shows hydrophobic interactions with His^{41} and Cys^{145} and hydrogen bonding interactions with Asn^{143} (Figure 2B), indicating that the docking site is located in the active center of Mpro SARS-CoV-2. The other comparison ligand, FJC, has ten pharmacophore features (Fig. 3A), including hydrogen bond donors, acceptors, and hydrophobic interactions.

The docking results reveal that FJC (Figure 3B) has a hydrophobic interaction with His^{41} and a hydrogen bond interaction with Cys^{145}. Based on visual analysis, it can be seen that LAK1, namely Cosmosiin derived from Asystasia Gangetica, has eight pharmacophore features familiar with alpha ketoamide (Figure 4A), including eight hydrophobic interactions. One of these interactions involves His^{41}.

LAK3, namely Glucobrassicin derived from Brassica oleracea, has seven pharmacophore features in common with Alpha ketoamide (Figure 5A). The results of re-docking (Figure 5B) show a hydrogen bond interaction with His41 and a hydrogen bond interaction with Cys^{145}. Meanwhile, LF3, namely Isobavachin derived from Psoralea corylifolia, has six pharmacophore features in common with FJC (Figure 6A) and 8 hydrogen interactions. One of these interactions involves Cys^{145} and six hydrophobic interactions (Figure 6B).

Visual analysis shows that LAK1, LAK3, and LF3 have interactions with residues in the catalytic center, indicating that they have the potential to effectively inhibit the activity of cutting non-structural proteins during the viral replication process.

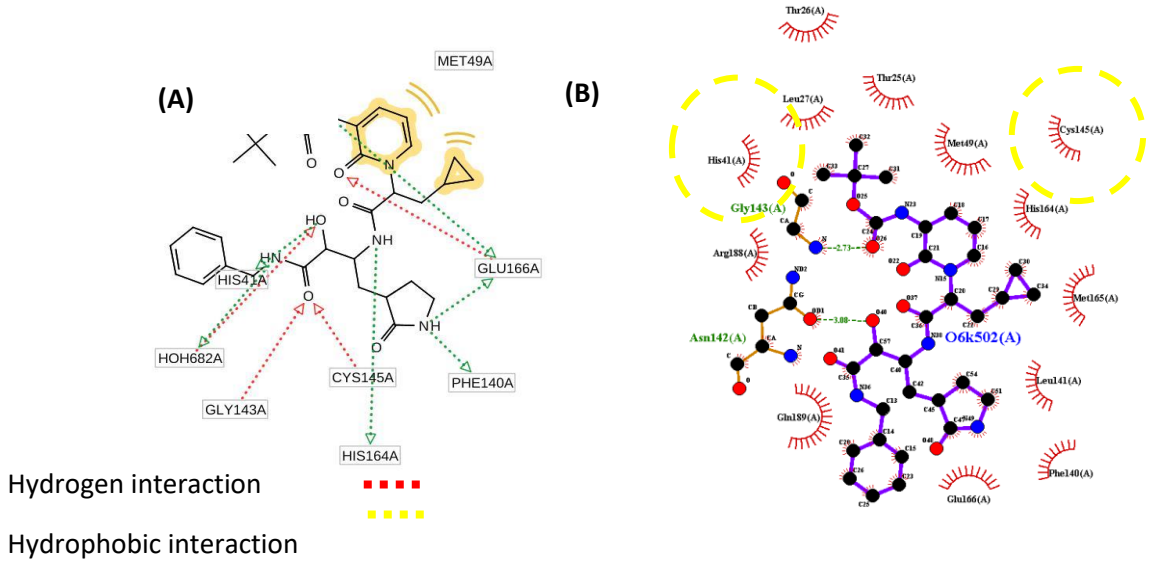

Figure 2 (A) Analysis of the pharmacophore features of Alpha ketoamide (B) Structure of the Alpha ketoamide Complex

http://jurnal.unpad.ac.id/ijcb

DOI: https://doi.org/10.24198/ijcb.v2i1.46021

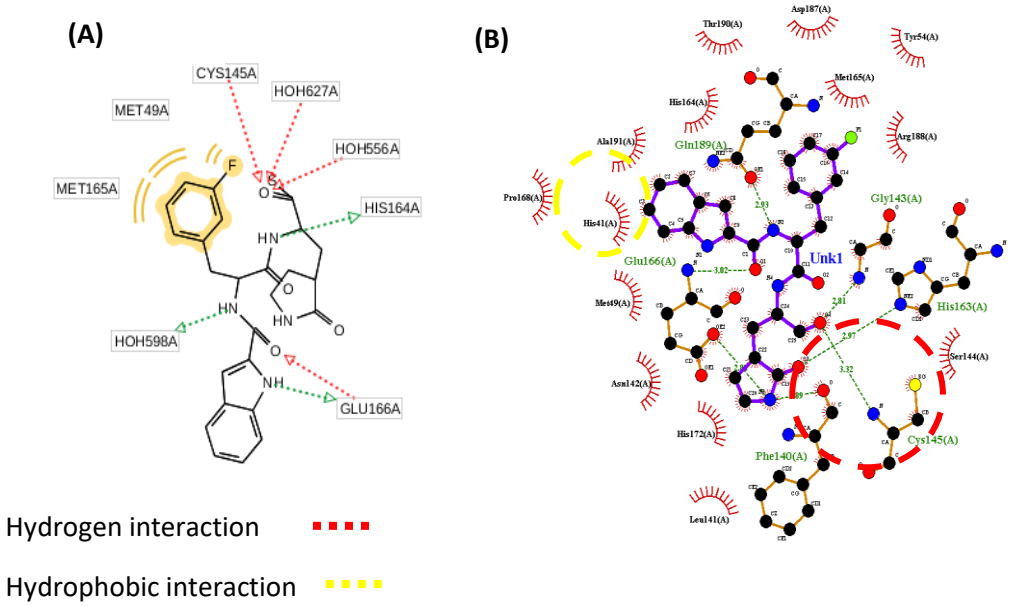

Figure 3 (A) Analysis of the pharmacophore features of FJC (B) Structure of the FJC Complex

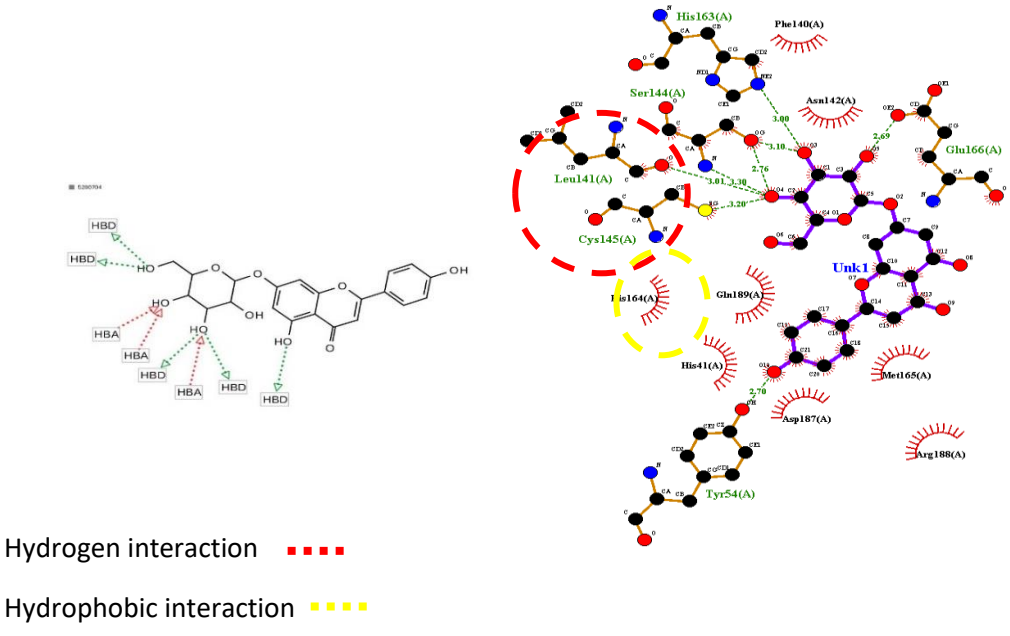

Figure 4 (A) Analysis of the pharmacophore features of LAK1 (B) Structure of the Complex LAK1

DOI: https://doi.org/10.24198/ijcb.v2i1.46021

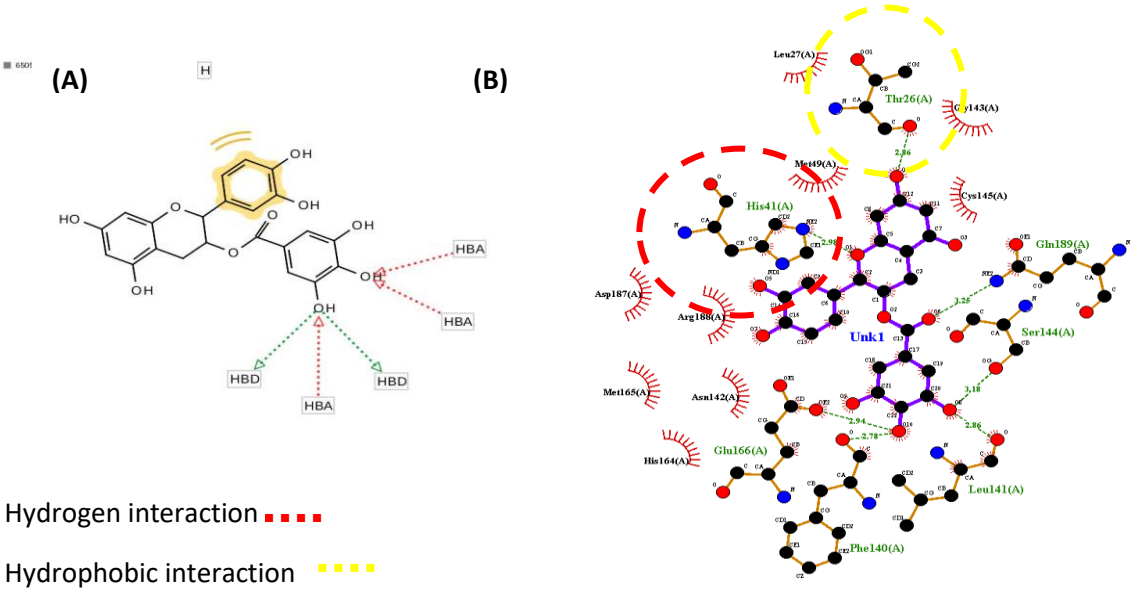

Figure 5 (A) Analysis of the pharmacophore features of LAK3 (B) Structure of the Complex LAK3

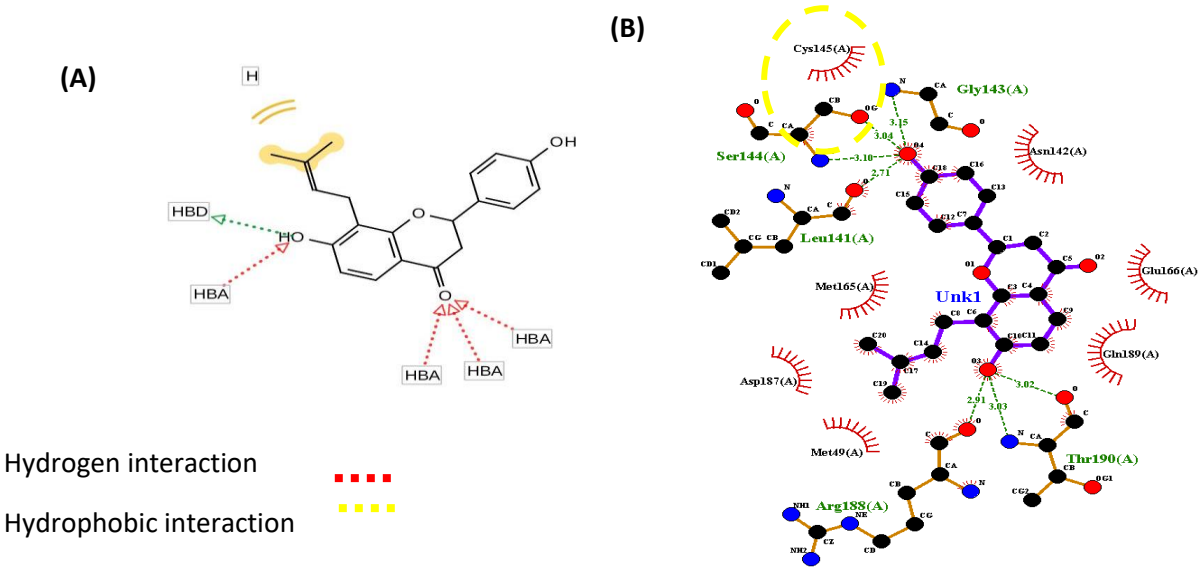

Figure 6 (A) Analysis of the pharmacophore features of LF3 (B) Structure of the Complex LF

The stability of the interaction of the complex structure can be validated using the Molecular Dynamics Simulation (MD) method which can show the stability of the structural conformation, the flexibility of the amino acid residues that are affected by docking, and the consistency of the appearance of hydrogen bonds during the simulation time. The MD method was applied to the ligands, LAK1, LAK3, and LF3. The convergence of the simulation of the complex structure is shown in Figure 7, the complex structure fluctuated sufficiently in the 50 ns time range, and the highest fluctuation occurred in LAK3, but the RMSD of the ligand (Figure 7B) showed that FJC and LAK3 best owned the stability of the ligand bond. The fluctuations of amino acid residues are shown in Figure 8. LAK3 has the highest average fluctuation value of 1.6 Å, which is consistent with the RMSD value of the LAK3 complex structure, which experienced a high value of changes in atomic displacement in the structure during the simulation. In comparison, the other complex structures have a relatively similar RMSF value of ~1 Å.

DOI: https://doi.org/10.24198/ijcb.v2i1.46021

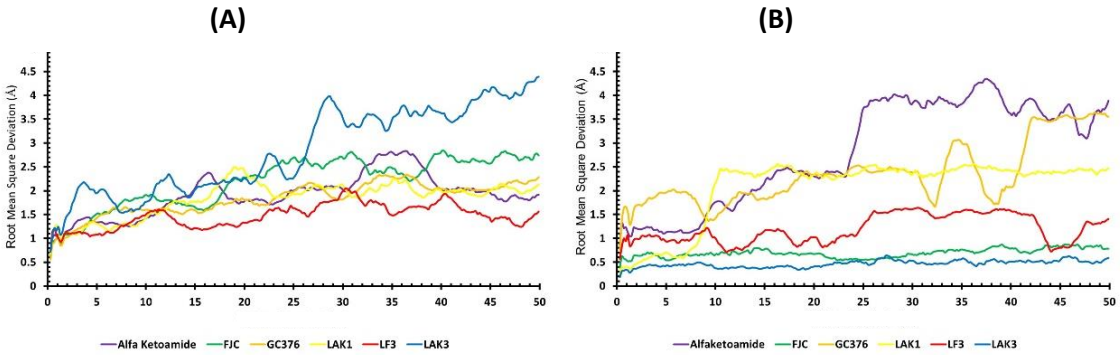

Figure 7 (A) RMSD Structure of Mpro Complex (Å) (B) RMSD Ligand (Å)

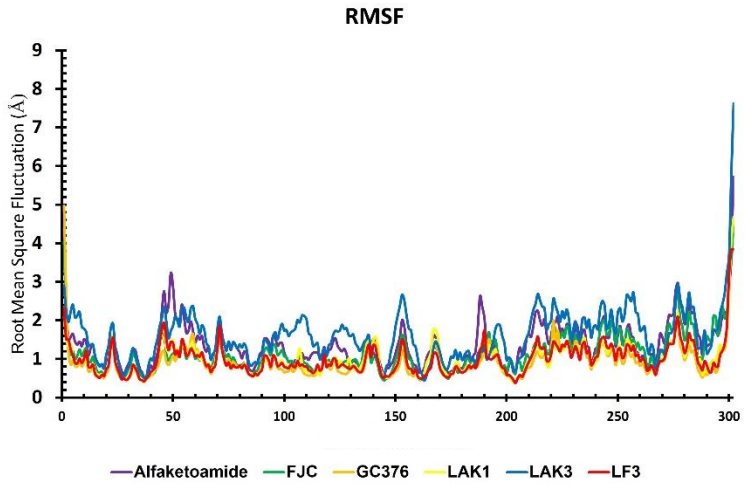

Figure 8 RMSF residues of amino acids Alpha ketoamide

Table 7 illustrates the presence of residual hydrogen bonds in the catalytic center and ligands throughout the simulation time. These include residues such as His[41], Gly[143], Cys145, and the oxyanion loop (residues 138–146), significantly cutting pp1a and pp1ab. Asn[142] forms a hydrogen bond acceptor with alpha ketoamide, while FJC shows several hydrogen bond donor interactions with Gly[143] and Cys[145] and a hydrogen acceptor with Phe[140]. GC376 displays donor interactions with His[41] and Gly[143].

Occupancy in hydrogen bonding refers to the extent or probability of a specific site or atom being involved in hydrogen bonding interactions. It indicates the likelihood of hydrogen bonds forming between a hydrogen bond donor and acceptor. The occupancy value provides information about the strength and frequency of hydrogen bonding interactions within a molecular system. Higher occupancy values indicate a higher likelihood of hydrogen bonding, while lower occupancy values suggest a weaker or less frequent occurrence of hydrogen bonding[20].

The natural compounds under investigation displayed favorable hydrogen bond interactions with the catalytic center (Table 7) Specifically, LAK1 exhibited donors Asn[142] and Gly[143] and acceptor His[41], while LAK3 had an acceptor interaction with Asn[142]. Conversely, LF3 shows no hydrogen bonding interactions, consistent with the docking simulation, which revealed only hydrophobic interactions (Figure 6).

The MMPBSA (Molecular Mechanics Poisson-Boltzmann Surface Area) method is a computational approach used to estimate the free energy changes associated with molecular systems. MMPBSA energy consists of several components contributing to the overall energy calculation, including electrostatic energy, van der Waals energy, and Poisson-Boltzmann (PB) solvation energy21. The ligand co-crystalize have higher MMPBSA energy values (Table 8) than the natural compounds, with values of -38.17 kcal/mol (Alpha ketoamide), -59.91 kcal/mol (FJC), and -43.12 kcal/mol (GC376). In comparison, Cosmosiin (LAK1) exhibited an MMPBSA energy value of -27.72 kcal/mol, Glucobrassicin (LAK3) of -38.81 kcal/mol, and Isobavachin (LF3) of 34.42 kcal/mol. Therefore, based on these findings, the natural compounds possess desirable properties and could be further explored for their potential therapeutic applications. Further in vitro and in vivo studies are needed to validate these results and determine the compounds' effectiveness in treating viral infections.

DOI: https://doi.org/10.24198/ijcb.v2i1.46021

Table 7 Hydrogen-bonded Mpro residues with Ligands

Ligan	Donor	Occupancy (%)	Acceptor	Occupancy (%)
Alpha Ketoamide	Gln^{192}	4.8	Asn^{142}	3.2
	Ser^{46}	2.8		
FJC	His^{163}	74.8	Gln^{189}	66.4
	Glu^{166}	40	Phe^{140}	26.4
	Cys^{145}	25.6	Glu^{166}	18
	Gly^{143}	12.8		
GC376	Glu^{166}	39.2	Gln^{189}	28.8
	His^{164}	23.2	Asp^{187}	20.4
	Gln^{192}	13.2		
	His^{41}	8		
	Gly^{143}	5.2		
LAK1	Asn^{142}	6.4	Asp^{187}	43.2
	Gly^{143}	5.6	Glu^{166}	61.6
			His^{41}	3.2
LAK3	His^{163}	16.4	Glu^{166}	81.2
			HIS^{164}	43.2
			Asn^{142}	25.6
LF3	His^{163}	10.8	Arg^{187}	41.2
			Thr^{189}	8

Table 8 Binding Energy of MMPBSA Complex Mpro (kcal/mol) for 50 ns taken every 200 frames.

Ligand	E(ele)	E(vdw)	E(PB)	E(PBSR)	MMPBSA
Alpha ketoamide	-3.53	-39.32	8.72	-4.04	-38.17
FJC	-9.45	-60.4	14.9	-5	-59.91
GC376	-7.6	-44.54	13.29	-4.27	-43.12
LAK1	-7.64	-27.64	10.78	-3.23	-27.72
LAK3	-13.18	-36.64	15.16	-4.14	-38.81
LF3	-4.14	-35.39	8.554	-3.44	-34.42

http://jurnal.unpad.ac.id/ijcb

DOI: https://doi.org/10.24198/ijcb.v2i1.46021

Conclusion

The simulation results suggest that the natural compounds cosmosiin, glucobrassicin, and isobavachin possess pharmacophore features, docking simulations, intramolecular interactions, molecular dynamics simulations, and ADMET properties similar to those of known Mpro inhibitors. These findings indicate that these natural compounds hold promise as potential inhibitors of SARS-CoV-2. However, further in vitro and in vivo studies must confirm their efficacy and safety as SARS-CoV-2 inhibitors. These studies could involve testing the compounds' inhibitory activity against SARS-CoV-2 in vitro and evaluating their pharmacokinetic and toxicological profiles in vivo. In summary, these natural compounds represent an interesting avenue for developing new therapeutics against SARS-CoV-2.

References

1. Chen N, Zhang B, Deng L, Liang B, Ping J. Virus-host interaction networks as new antiviral drug targets for IAV and SARS-CoV-2. *Emerg Microbes Infect*. 2022;11(1):1371. doi:10.1080/22221751.2022.2071175

2. Kondylis V, Kumari S, Vlantis K, Pasparakis M. The interplay of IKK, NF-κB and RIPK1 signaling in the regulation of cell death, tissue homeostasis and inflammation. *Immunol Rev*. 2017;277(1):113-127. doi:10.1111/IMR.12550

3. Dai W, Zhang B, Jiang XM, et al. Structure-based design of antiviral drug candidates targeting the SARS-CoV-2 main protease. *Science*. 2020;368(6497):1331-1335. doi:10.1126/SCIENCE.ABB4489

4. Antonopoulou I, Sapountzaki E, Rova U, Christakopoulos P. Inhibition of the main protease of SARS-CoV-2 (Mpro) by repurposing/designing drug-like substances and utilizing nature's toolbox of bioactive compounds. *Comput Struct Biotechnol J*. 2022;20:1306. doi:10.1016/J.CSBJ.2022.03.009

5. Erlina L, Paramita RI, Kusuma WA, et al. Virtual screening of Indonesian herbal compounds as COVID-19 supportive therapy: machine learning and pharmacophore modeling approaches. *BMC Complement Med Ther*. 2022;22(1):1-19. doi:10.1186/S12906-022-03686-Y/FIGURES/7

6. Syahdi RR, Iqbal JT, Munim A, Yanuar A. HerbalDB 2.0: Optimization of construction of three-dimensional chemical compound structures to update Indonesian medicinal plant database. *Pharmacognosy Journal*. 2019;11(6):1189-1194. doi:10.5530/PJ.2019.11.184

7. Yang H, Lou C, Sun L, et al. admetSAR 2.0: web-service for prediction and optimization of chemical ADMET properties. *Bioinformatics*. 2019;35(6):1067-1069. doi:10.1093/BIOINFORMATICS/BTY707

8. Neese F. Software update: the ORCA program system, version 4.0. *Wiley Interdiscip Rev Comput Mol Sci*. 2018;8(1):e1327. doi:10.1002/WCMS.1327

9. Case DA, Cheatham Iii TE, Darden T, et al. *The Amber Biomolecular Simulation Programs*. http://amber.scripps.edu.

10. Meller J. Molecular Dynamics. *eLS*. Published online April 19, 2001. doi:10.1038/NPG.ELS.0003048

11. Dai W, Zhang B, Jiang XM, et al. *Structure-Based Design of Antiviral Drug Candidates Targeting the SARS-CoV-2 Main Protease*.

12. Vuong W, Khan MB, Fischer C, et al. Feline coronavirus drug inhibits the main protease of SARS-CoV-2 and blocks virus replication. *Nature Communications 2020 11:1*. 2020;11(1):1-8. doi:10.1038/s41467-020-18096-2

13. Zhang L, Lin D, Sun X, et al. Crystal structure of SARS-CoV-2 main protease provides a basis for design of improved α-ketoamide inhibitors. *Science*. 2020;368(6489):409-412. doi:10.1126/SCIENCE.ABB3405

14. Lensink MF, Méndez R, Wodak SJ. Docking and scoring protein complexes: CAPRI 3rd Edition. *Proteins*. 2007;69(4):704-718. doi:10.1002/PROT.21804

15. Nguyen NT, Nguyen TH, Pham TNH, et al. Autodock Vina Adopts More Accurate Binding Poses but Autodock4 Forms Better Binding Affinity. *J Chem Inf Model*. 2020;60(1):204-211. doi:10.1021/ACS.JCIM.9B00778/SUPPL_FILE/CI9B00778_SI_001.PDF

16. Wessel M, Mente S. Chapter 25. ADME by computer. *Annual Reports in Medicinal Chemistry - ANNU REP MED CHEM*. 2001;36:257-266. doi:10.1016/S0065-7743(01)36065-7

17. Cheng F, Li W, Zhou Y, et al. AdmetSAR: A comprehensive source and free tool for assessment of chemical ADMET properties. *J Chem Inf Model*. 2012;52(11):3099-3105. doi:10.1021/CI300367A/SUPPL_FILE/CI300367A_SI_001.PDF

18. Ng MCK, Fong S, Siu SWI. PSOVina: The hybrid particle swarm optimization algorithm for protein–ligand docking. *https://doi.org/101142/S0219720015410073*. 2015;13(3). doi:10.1142/S0219720015410073

19. Zheng K, Ma G, Zhou J, et al. Insight into the activity of SARS main protease: Molecular dynamics study of dimeric and monomeric form of enzyme. *Proteins*. 2007;66(2):467-479. doi:10.1002/PROT.21160

20. Padhi AK, Kumar H, Vasaikar S V., Jayaram B, Gomes J. Mechanisms of loss of functions of human angiogenin variants implicated in amyotrophic lateral sclerosis. *PLoS One*. 2012;7(2). doi:10.1371/JOURNAL.PONE.0032479

21. Homeyer N, Gohlke H. Free energy calculations by the Molecular Mechanics Poisson-Boltzmann Surface Area method. *Mol Inform*. 2012;31(2):114-122. doi:10.1002/MINF.201100135